Supporting Information:

Creating Molecular-Scale Graded Electronic Profile in Single Polymer to Facilitate Hole Injection for Efficient Blue Electroluminescence**

By *Chih-Wei Huang, Kang-Yung Peng, Ching-Yang Liu, Tzu-Hao Jen, Neng-Jye Yang and Show-An Chen**

A. The Synthesis Procedures and Characterization for the Monomers and Polymers:

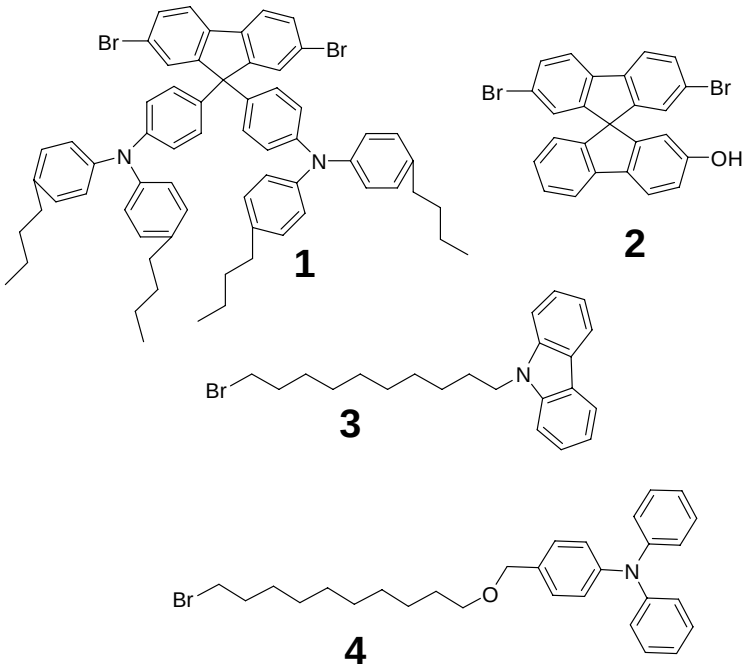

9,9-Bis(4-di(4-butylphenyl)aminophenyl)-2,7-dibromofluorene **1** [S1], 2,7-dibromo-2'-hydroxy-9,9'-spirobifluorene **2** [S2], 9-(10-bromodecyl)-9H-carbazole **3** [S3] and 4-((10-bromodecyloxy)methyl)-*N*,*N*-diphenylbenzenamine **4** [S4] were synthesized in accordance with the literature.

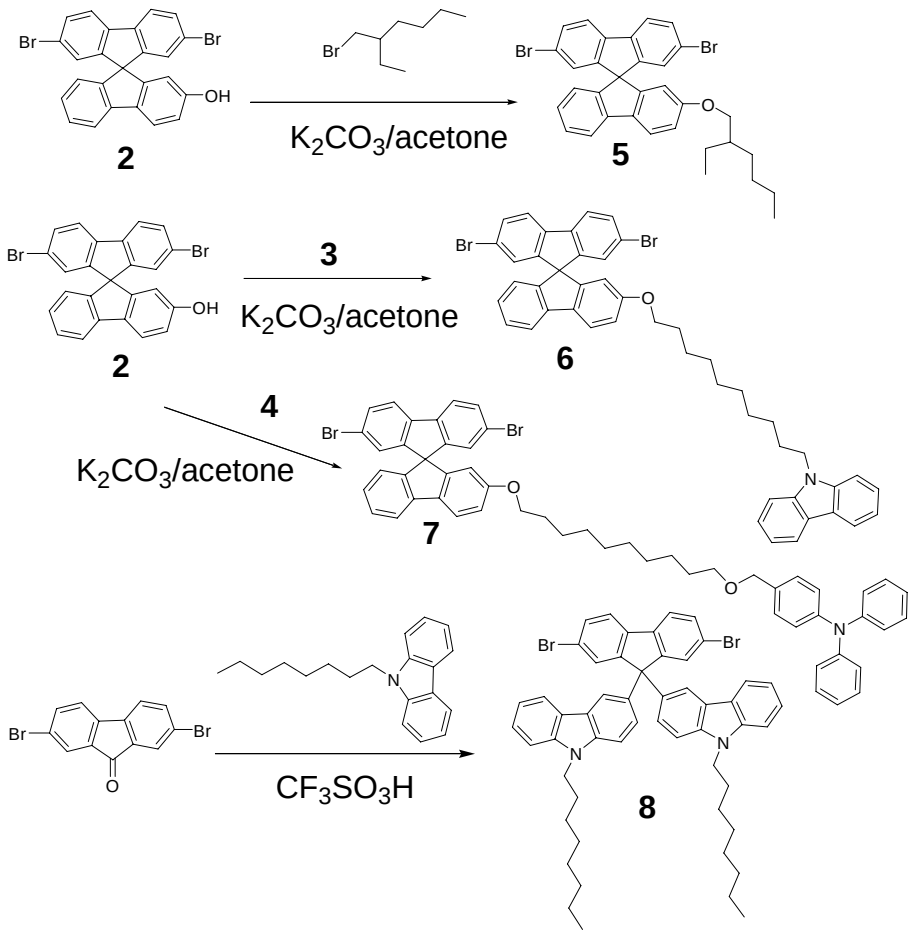

2,7-dibromo-2'-ethylhexyl-9,9'-spirobifluorene (5)

A mixture of **2** (2 g, 4.08 mmol), 1-bromoethylhexane (0.867 g, 4.49 mmol), K_2CO_3 (1.375 g, 10.37 mmol) and 18-crown-6 (7.5 mg) in dry acetone was heated to reflux and stirred vigorously under nitrogen overnight. After removing the solvent, the reaction residue was partitioned between water and CH_2Cl_2 phases; after separating the organic layers, the aqueous layer was extracted with CH_2Cl_2. The combined organic layer was dried over $MgSO_4$. Removed the solvent and the crude product was purified by column chromatography packed with silica gel eluting with hexane increasing to CH_2Cl_2/ hexane at 1:1 by volume to afford **5** as a white solid 2.33 g (95 %). ^{1}H NMR (400 MHz, $CDCl_3$) : δ7.73 (dd, 2H), 7.67 (d, 2H), 7.49 (dd, 2H), 7.36 (t,1H), 7.06 (t, 1H), 6.94 (dd, 1H), 6.86 (d, 2H), 6.65 (d, 1H), 6.22 (d, 2H), 3.69 (t, 2H), 1.57 (m, 1H), 1.37 (m, 8H), 0.85 (t, 6H) ; ^{13}C NMR (100MHz, $CDCl_3$): δ 159.9, 150.8, 148.7, 146.7, 141.8, 139.6, 134.3, 131.1, 128.2, 127.5, 126.8, 123.8, 121.9, 121.3, 121.0,

119.3, 114.5, 110.4, 70.8, 65.6. 39.5, 30.5, 29.1, 23.8, 23.0, 14.0, 11.1 LR-MS(FAB) calculated $C_{33}H_{30}Br_2O$: m/z = 602.40. Found: m/z = 602.

2,7-dibromo-2'-N-carbazolyl-decyl-9,9'-spirobifluorene (6)

A mixture of **2** (2 g, 4.08 mmol), 9-(10-bromodecyl)-9H-carbazole (1.73 g, 4.49 mmol), K_2CO_3 (1.375 g, 10.37 mmol) and 18-crown-6 (7.5 mg) in dry acetone was heated to reflux and stirred vigorously under nitrogen overnight. After removing the solvent, the reaction residue was partitioned between water and CH_2Cl_2 phases; after separating the organic layers, the aqueous layer was extracted with CH_2Cl_2. The combined organic layer was dried over $MgSO_4$. Removed the solvent and the crude product was purified by column chromatography packed with silica gel eluting with hexane increasing to CH_2Cl_2/ hexane to 3:1 to afford **6** as a white solid 2.92 g (90 %). ^{1}H NMR (400 MHz, $CDCl_3$) : δ 8.07 (d, 2H), 7.71 (m, 2H), 7.62 (d, 2H), 7.36 (m, 7H), 7.19 (td, 2H), 7.04 (td, 1H), 6.90 (dd, 1H), 6.83 (d, 2H), 6.64 (d, 1H), 6.20 (d, 1H), 4.28 (t, 2H), 3.78 (t, 2H), 1.83 (m, 2H), 1.62 (m, 2H), 1.32~1.12 (m, 12H); ^{13}C NMR (100MHz, $CDCl_3$): δ 159.6, 150.8, 148.8, 146.6, 141.8, 140.4, 139.6, 134.4. 131.1, 120.2, 127.4, 126.8, 125.5, 123.9, 122.8, 121.9, 121.3, 121.0, 120.3, 119.4, 118.7, 114.4, 110.3, 108.6, 68.1, 65.6, 43.1, 29.3, 29.3, 29.0, 27.3, 26.0 LR-MS(FAB) calculated $C_{47}H_{41}Br_2NO$: m/z = 795.64. Found: m/z = 795.

2,7-dibromo-2'-4-((10-bromodecyloxy)methyl)-*N*,*N*-diphenylbenzenamine-9,9'-spirobifluorene (7)

A mixture of **2** (2g, 4.08 mmol), 4-((10-bromodecyloxy)methyl)-*N*,*N*-diphenylbenzenamine (2.22g, 4.49mmol), K_2CO_3 (1.375 g, 10.37mmol) and 18-crown-6 (7.5mg) in dry acetone was heated to reflux and stirred vigorously under nitrogen overnight. After removing the solvent, the reaction residue was partitioned between water and CH_2Cl_2 phases; after separating the organic layers, the aqueous layer was extracted with CH_2Cl_2. The combined organic layer was dried over $MgSO_4$. Removed the solvent and

the crude product was purified by column chromatography packed with silica gel eluting with hexane increasing to CH_2Cl_2/ hexane to to afford **7** as a white solid 3.44g (85 %). ^{1}H NMR (400 MHz, $CDCl_3$) : δ 7.71 (t, 2H), 7.63 (d, 2H), 7.46 (dd, 2H), 7.34 (t, 1H), 7.21 (m, 6H), 7.04 (t, 6H), 6.97 (t, 2H), 6.91 (dd, 2H), 6.83 (s, 2H), 6.64 (d, 1H), 6.20 (d, 1H), 4.41 (s, 2H), 3.78 (t, 2H), 3.45 (t, 2H), 1.62 (m, 4H) 1.32 (m, 12H) ^{13}C NMR (100MHz, $CDCl_3$): δ 159.59, 150.75, 148.76, 147.78, 147.18, 146.60, 141.73, 139.54, 134.31, 132.89, 131.07, 129.15, 128.81, 128.21, 127.39, 126.79, 123.99, 122.63, 121.32, 120.97, 119.38, 114.36, 110.25, 72.57, 70.57, 68.13, 65.55, 29.72, 29.42, 29.34, 29.24, 26.15, 25.96 LR-MS(FAB) calculated $C_{54}H_{49}Br_2NO_2$: m/z = 903.78. Found: m/z = 903.

9,9-Bis(3,3'- N-octyl-9H-carbazole)-2,7-dibromofluorene (8)

To a misxture of 2,7-dibromofluorenone (3.15g, 9.31mmol) and 9-octyl-9H-carbazole (7.80g, 27.93mmol) were added methanesulfonic acid (600μL, 0.93mmol). The reation mixture was heated at 90℃ under inert atmosphere overnight. The cooled mixture was quenched by aqueous sodium carbonate and extrated with CH_2Cl_2, The combined organic layer was dried over $MgSO_4$. Removed the solvent and the crude product was purified by column chromatography packed with silica gel eluting with hexane increasing to CH_2Cl_2/ hexane to afford **8** as a slight yellow crystal 2.69g (33 %). ^{1}H NMR (400 MHz, $CDCl_3$) : δ 8.07 (d, 2H), 8.01 (d, 2H), 7.79 (s, 2H), 7.65 (d, 2H), 7.55 (d, 2H), 7.47 (m, 4H), 7.32 (d, 2H), 7.21 (d, 2H), 4.25 (t, 4H), 1.88 (m, 4H), 1.36 (m, 20H), 0.98 (t, 6H); ^{13}C NMR (100MHz, $CDCl_3$): δ 154.62, 140.74, 139.43, 137.93, 135.43, 130.63, 129.63, 126.05, 125.66, 122.64, 122.54, 121.78, 121.53, 120.42, 119.50, 118.68, 108.68, 108.63, 65.88, 43.03, 31.75, 31.56, 29.31, 29.12, 18.96, 27.25, 22.63, 22.57, 14.11, 14.06 LR-MS(FAB) calculated $C_{53}H_{54}Br_2N_2$: m/z = 878.81. Found: m/z = 878.

General procedure of polymerization for spiro-polyfluorene by the Yamamoto coupling reaction, taking Cz-TPA-sPF as an example.

Into a reactor, bis(1,5-cyclooctadiene) nickel (0) ($Ni(COD)_2$) (0.438 g, 1.59 mmol), 2,2-bipyridyl (BPY) (0.249 g, 1.59 mmol), 1,5-cyclooctadiene (COD) (0.172 g, 1.59 mmol) and anhydrous DMF (3.75 mL) were added in a glove box with nitrogen. This mixture was stirred at 90℃ for 30 min to form active catalyst. The monomer **1** (500 mg) and **5** (384 mg) in 11.25 mL of anhydrous toluene was added to the mixture. The polymerization proceeded at 85 ℃ for 2 days in the glove box, and then 1-bromo-4-tert-butylbenzene (TBP, from Sigma-Aldrich) as end-capping agent (16.5 μL) was added and allowed the mixture to react for 24 h more. The resulting polymer was purified by alumina oxide chromatography, precipitated in acetone/methanol (volume ratio=1:1) and finally dried under vacuum for 24 h to obtain the polymer.

Determination of actual ratio units in copolymers

We calculate the actual ratio units in copolymers from NMR spectra. Taking TPA-Cz-sPF as an example, see Fig. 2. The chemical shift in δ4. 379 represent the proton in the 2 position (2H, next to the TPA ring of monomer 7); the chemical shift in δ4.146 represents the character of proton in the 1 position (4H, next to nitrogen atom of the Cz ring of monomer 8). By compared to the integrated values of each proton of 1 and 2 position (0.4147 for each proton in 1, 0.445 for each in 2), we can determine the actual ratio of the monomer 7 and 8. In this case, the approximate content of monomer 7 is 0.445/(0.4174+0.445) (that is ca. 0.52). Therefore, we can determine the actual ratio of the monomer 7 and 8. The actual composition of monomer 7 and 8 in TPA-Cz-sPF is 52% and 48%, respectively.

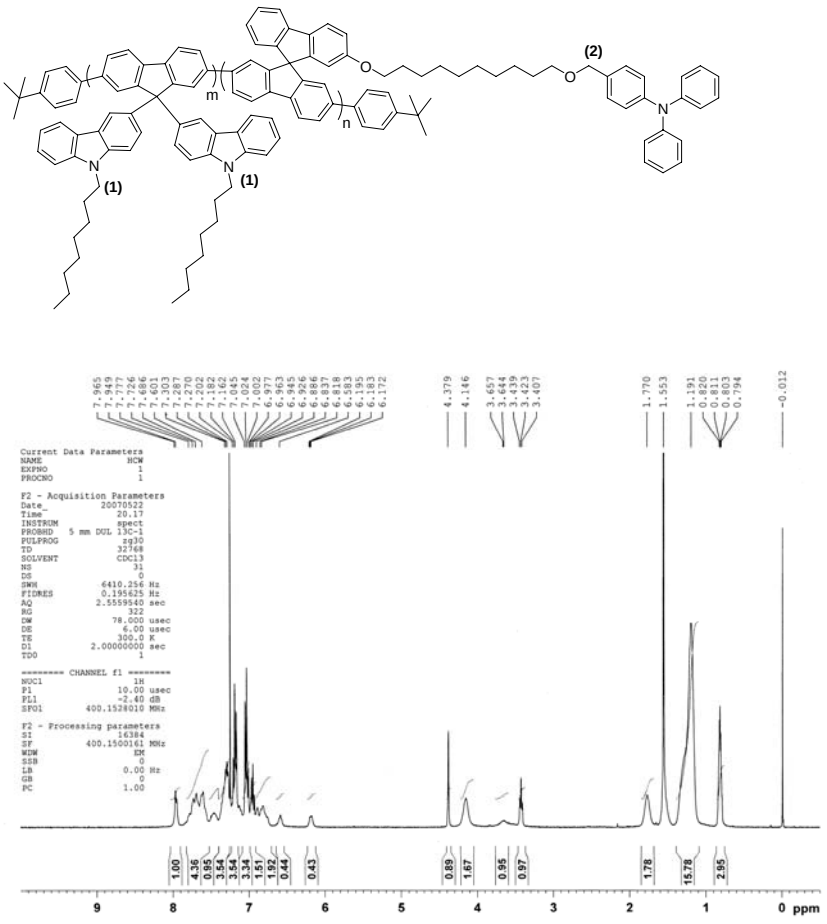

Figure S1. Determination of actual content of monomers in TPA-Cz-sPF.

Yield of sPF: 40%. ^{1}H NMR (400 MHz, $CDCl_3$): δ 7.64 (m, 4H), 7.24 (m, 2H), 6.83 (m, 3H), 6.60 (m, 1H), 6.16 (m, 1H), 3.57 (m, 2H), 1.54 (m, 1H), 1.15 (m, 8H), 0.75 (m, 6H). Anal. Calcd. C, 89.15; H, 7.25. Found: C, 89.14; H, 6.89

Yield of TPA50-sPF: 63%. ^{1}H NMR (400 MHz, $CDCl_3$): δ 7.67 (m, 4H), 7.51 (m, 2H), 6.98 (m, 12H), 6.74 (m, 4H), 6.20 (m, 1H), 3.61 (m, 2H), 2.47 (m, H), 1.54 (m, 5H), 1.32 (m, 17H), 1.24 (m, 6H), 1.54 (m, 3H), 1.15 (m, 6H), 0.75 (m, 3H). The content of monomer **1** is around 37% by mole. Anal. Calcd. N, 2.12; C, 89.18; H, 7.48. Found: N, 2.60; C, 89.07; H, 7.36

Yield of TPA100-sPF: 30%. ^{1}H NMR (400 MHz, $CDCl_3$): δ 7.77 (m, 1H), 7.59 (m, 3H), 7.02 (m, 4H), 6.94 (m, 16H), 6.76 (m, 6H), 2.51 (m, 8H), 1.50 (m, 8H), 1.29 (m, 8H), 0.88 (m, 12H). Anal. Calcd. N, 3.19; C, 88.99; H, 7.81. Found: N, 3.56; C, 87.74; H, 7.76

Yield of Cz50-sPF: 35%. ^{1}H NMR (400 MHz, $CDCl_3$): δ 8.07 (m, 2H), 7.63 (m, 7H), 7.35 (m, 5H), 7.20 (m, 2H), 6.83 (m, 7H), 6.66 (m, 2H), 6.16 (m, 2H), 4.22 (m, 4H), 3.61 (m, 4H), 1.84 (m, 5H), 1.23 (m, 17H), 0.82 (m, 6H). The content of monomer **5** is around 50% by mole. Anal. Calcd. N, 1.30; C, 88.93; H, 6.81. Found: N, 1.11; C, 89.83; H, 6.10

Yield of Cz100-sPF: 25%. ^{1}H NMR (400 MHz, $CDCl_3$): δ 8.07 (m, 2H), 7.64 (m, 4H), 7.40 (m, 7H), 7.24 (m, 2H), 6.83 (m, 3H), 6.61 (m, 1H), 6.16 (m, 1H), 4.22 (m, 2H), 3.61 (m, 2H), 1.74 (m, 4H), 0.90 (m, 16H). Anal. Calcd. N, 2.10; C, 88.38; H, 7.11. Found: N, 2.31; C, 89.33; H, 7.10

Yield of Cz-TPA-sPF: 73%. ^{1}H NMR (400 MHz, $CDCl_3$): δ 8.07 (m, 2H), 7.68 (m, 5H), 7.52 (m, 4H), 7.39 (m, 5H), 7.24 (m, 3H), 7.06 (m, 23H), 6.77 (m, 5H), 6.26 (m, 1H), 4.22 (m, 1H), 3.74 (m, 1H), 2.55 (m, 8H), 1.80 (m, 2H), 1.54 (m, 18H), 1.41 (m, 14H), 1.37 (m, 6H), 0.93 (m, 11H). The content of monomer **1** is around 47% by mole. Anal. Calcd. N, 2.78; C, 88.90; H, 7.26. Found: N, 2.63; C, 88.55; H, 7.19

Yield of TPA-Cz-sPF: 52%. ^{1}H NMR (400 MHz, $CDCl_3$): δ 7.96 (m, 2H), 7.71 (m, 9H), 7.29 (m, 2H), 7.18 (m, 7H), 7.02 (m, 7H), 6.96 (m, 7H), 6.83 (m, 4H), 6.58 (m, 1H), 6.18 (m, 1H), 4.38 (m, 2H), 4.15 (m, 4H), 3.65 (m, 2H), 3.42 (m, 2H), 1.77 (m, 4H), 1.19 (m, 30H), 0.807 (m, 6H). The content of monomer **8** is around 48% by mole. Anal. Calcd. N, 2.81; C, 87.68; H, 7.366. Found: N, 2.88; C, 87.83; H, 3.10

Table S1 Weight average molecular weights (Mw) and polydispersities(PDI) of poly-spiros

Polymer	Mw (10^4 Dalton)	PDI
sPF	11.0	2.2
TPA50-sPF	13.7	1.5
TPA100-sPF	4.7	2.3
Cz50-sPF	1.2	3.4
Cz100-sPF	1.4	2.0
Cz-TPA-sPF	16.0	2.1
TPA-Cz-sPF	19.0	2.0

Table S2 Comparison of feed ratio and actual content of co-monomers in the copolymers of poly-spiro [a]

Polymer	Feed Molar ratio	Actual Molar ratio found in polymers
TPA50-sPF	50% of **1**; 50% of **5**	37% of **1;** 67**%** of **5**
Cz50-sPF	50% of **5;** 50**%** of **6**	50% of **5;** 50**%** of **6**
TPA-Cz-sPF	50% of **7**; 50% of **8**	52% of **7**; 48% of **8**
Cz-TPA-sPF	50% of **1**; 50% of **6**	47% of **1**; 53% of **6**

[a]. Calculated from the NMR spectra.

B. Cyclic Voltammetry of Poly-spiros:

Cyclic voltammetry (CV) of the polymer films coated on the ITO glass was conducted in an electrolyte of 0.1 M tetrabutylamminonium hexafluorophosphate ($TBAPF_6$) in acetonitrile using ferrocene as the standard. Figure S2 shows the results from CV measurement for the poly-spiros with graded hole-transporting pendant groups. While grafting Cz moiety spaced by alkoxy group and TPA onto the backbone of poly-spiros, Cz-TPA-sPF, three oxidation peaks (their onset potentials are 0.90, 1.13 and 1.33 V, which are referred to TPA, Cz and poly-spiro backbone, respectively) are observed during the anodic scan (due to the difficulty in identification of onset potentials between Cz and backbone, the oxidation potential of backbone can also be determined by sPF). Each individual oxidation potential peak has its corresponding absorption peak in the UV-Vis. By use of the results of CV together with the UV-visble spectra, the energy diagram of poly-spiro can be determined (in the inset of Fig. 1b). For Cz-TPA-sPF, which possesses the three step descent HOMO levels: 5.3 (for TPA), 5.5 (for Cz) and 5.7 eV (for backbone), allowing holes injected from the anode to transport through the interface to LEPs via three descending HOMO levels.

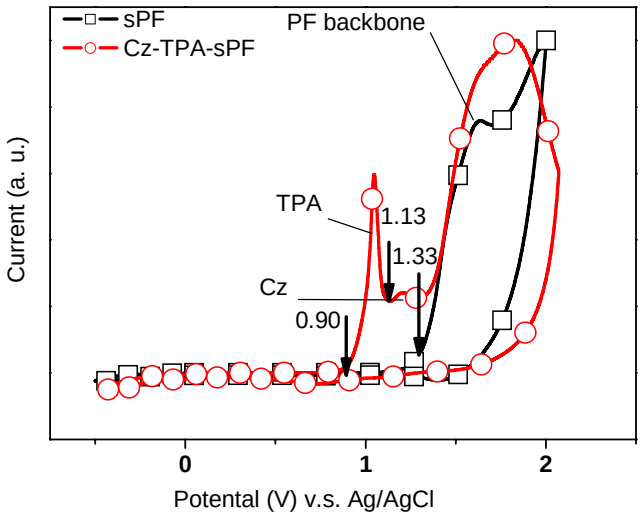

Figure S2. Cyclic voltammetry measurements of poly-spiros, demonstrating that each hole-transporting moiety possesses an independent oxidation potential peak as the main chain. The arrows indicate the onsets of the corresponding oxidation peaks.

C. Summary of Device Performance of the Present Poly-spiros :

Table S3. Summary of device performances based on the present poly-spiros [a].

Polymer	Brightness (cd/m2)	Efficiency cd/A (%)	CIE (x, y)@6V	Turn-on Voltage (V_{on})[b]
sPF	10,000@8.5V	0.96 (1.10)@4.0V	(0.16, 0.09)	3.3
TPA50-sPF	13,000@9.0V	2.02 (2.79)@3.8V	(0.16, 0.07)	2.8
TPA100-sPF	7,500@7.7V	3.76 (3.54)@4.6V	(0.16, 0.11)	2.8
Cz50-sPF	12,000@9.5V	1.39 (1.90)@4.3V	(0.16, 0.07)	3.1
Cz100-sPF	6,500@8.0V	1.54 (2.11)@4.3V	(0.16, 0.07)	3.1
Cz-TPA-sPF	22,000@8.5V	4.57 (4.54)@3.8V	(0.16, 0.10)	2.8
TPA-Cz-sPF	14,000@6.1V	13.10 (7.53)@3.7V	(0.19, 0.21)	2.9

a. The device structure is ITO/PEDOT/poly-spiros/CsF/Ca/Al.

b. The turn-on voltage is defined as that the brightness starts to be over 0.2 Cd/m^2.

D. Spatial sequence of graded electronic profile demonstrated from surface analyses

X-ray photoelectron spectroscopy (XPS) measurement. All polymers were spin coated on PEDOT:PSS-coated ITO substrate from their dilute solutions in THF (about 1.5 mg/ml) to form films of 15-25 nm thick. Prior to spin coating, ITO was washed successively in an ultrasonic cleaner in isopropyl alcohol, acetone, NH_4OH/H_2O_2, and de-ionized water, followed by a routine oxygen plasma treatment. PEDOT:PSS (about 20 nm) was then spin coated onto the treated ITO and subsequently baked at 140 °C under vacuum for one hour. The PEDOT:PSS solution used is Baytron AI 4083 from Bayer and its solid film coated on ITO is considered as a polymer electrode. The samples for XPS analysis were handled in a glove box with nitrogen and moved into a desiccator. The whole assembly was taken out from the glove box, and the XPS samples were then transferred quickly (in less than 10 s) in air to the sample loading chamber. Such transferring process would minimize possible influence by an exposure to air.

Figure S3 shows the XPS spectra (from Thermo Electron Corporation) of investigated poly-spiros coated onto ITO. By integrating the areas of peaks in the spectra, we can determine the atom contents of the poly-spiros on the surface (within 3.0 nm) and the results are list in Table S4. For TPA-Cz-sPF, the content of oxygen atom increases from 1.79% in the bulk to 2.90% on the surface, indicating that more TPA groups appear on the surface than those in the bulk by a factor of 1.62 (since the oxygen atom only attached on TPA moiety in this case). In other words, the distributions of moieties in the poly-spiros on the surface are quite different from those in the bulk.

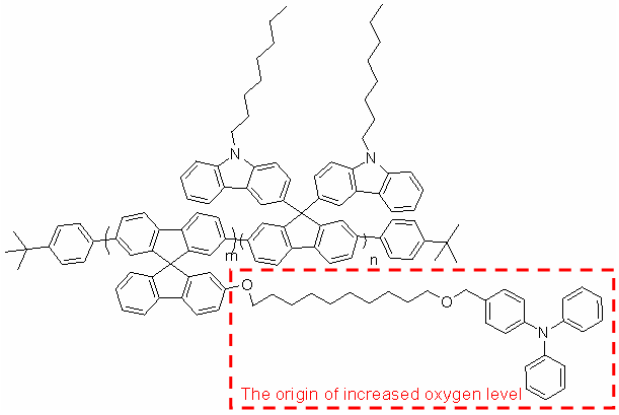

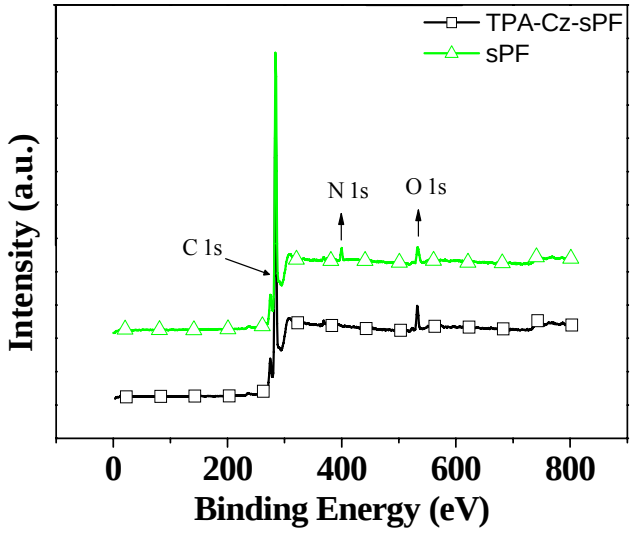

FIGURE S3 XPS spectra of sPF and TPA-Cz-sPF

Table S4. Surface and bulk atom content of TPA-Cz-sPF

	C%	N%	O%
TPA-Cz-sPF (surface) [a]	94.63	2.47	**2.90**
TPA-Cz-sPF (bulk) [b]	95.53	2.68	**1.79**

[a] within the depth of x-ray surface analysis, about 3 nm.

[b] calculated from the chemical structure

The result of XPS analysis shows that the content of TPA moiety with long spacer in TPA-Cz-sPF at the interface is much higher than that in the bulk by ca. 62%, which was calculated from the increased oxygen level, (2.90-1.79)/1.79). In other words, TPA has more chance to be in contact with the anode and cathode than Cz that linked directly to the backbone. This fact can be attributed to the flexibility of TPA side chains with alkoxyl linkage in TPA-Cz-sPF, allowing the side chain to extend to the surface easier than Cz moiety directly attached to main chain.

E. Graded electronic profile demonstrated by photoexcitation dynamics analysis

Due to the process of cascade hole injection from PEDOT, TPA, Cz and finally to main chain does not emit light, we can not verify the process directly. However, we can use time-resolve photoluminescence spectroscopy of poly-spiros to examine the process indirectly. The photoluminescence decay curves of polymers were measured by a time-correlated single photon counting (TCSPC) system with a microchannel plate photomultiplier tube (Hamamatsu Photonics R3809U-50) and a spectrometer (Edinburgh,Lifespec-ps with TCC900 data acquisition card). Excitation pulse for the TCSPC experiments was provided by a frequency doubled output (harmonic generator, Inrad 5-050) of a modelocked Ti-Sapphire laser (Coherent Mira-900) pumped by a diode laser (Coherent Verdi-V10). The repetition rate was reduced to 4 MHz by a pulse picker (Coherent Mira 9200) between Mira-900 and In-rad 5050.

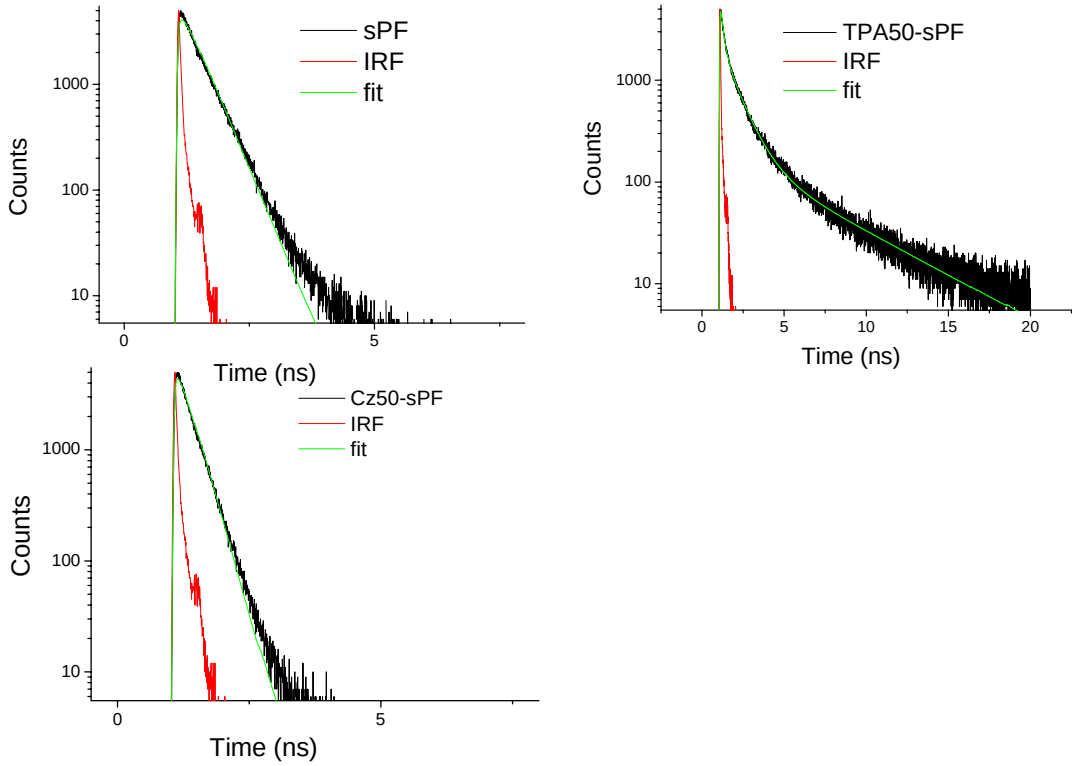

FIGURE S5 Luminescence decays of emission from sPF, TPA50-sPF and Cz50-sPF.

Fig. S5 shows the time-resolved luminescence decay curves of sPF, TPA50-sPF and Cz50-sPF (excitation at 390 nm, i.e. main chain; collected at 424 nm). The decay constants (τ) of the luminescence and the square of the correlation coefficients (R^2) of the exponential fitting for each curve are listed in Table S5. The decay constant of sPF is 374 ps, very close to the reported value (320 ps) in Ref. [S5], while that of TPA50-sPF (132 ps) and Cz50-sPF (245 ps) are much shorter, indicating that TPA and Cz groups can increase the exciton dissociation rate. Three components of the emissive lifetime for TPA50-sPF were observed. The first one can be attributed to exciton relaxation from main chain (132 ps, 72%); the second one, to exciton dissociation by TPA then recombined in main chain (928 ps, 25%); the third one, to exciton dissociation by TPA dimer (Ref. [S6]) then recombined in main chain (4889 ps, 3%). As for TPA50-sPF (132 ps) and Cz50-sPF (245 ps), TPA possesses stronger exciton dissociation capability than Cz. That is, when exciton is formed on the main chain after excitation, TPA can dissociate exciton (i.e. trap hole) in the main chain more efficient than Cz. Thus, the "dissociation capabilities" of the TPA and Cz can be taken as their "hole trapping capabilities". Therefore, from the energetic point of view, when hole injected from anode (PEDOT) in the LEDs, it would hop to TPA much easier than to Cz or main chain (TPA exhibits the strongest hole trapping capability) if spatially allowed. Further hopping from TPA to Cz is much easier than to main chain due to stronger hole trapping capability of Cz. Finally, the hole in Cz would hop into main chain to emit blue light after recombination with an electron there. Also, from the results of CV measurements for poly-spiros in SI part B, the sequence of oxidation potential is TPA< Cz< main chain, which also provides a support on the sequential cascade injection in Cz-TPA-sPF and TPA-Cz-sPF.

Table S5 Decay constant (τ) of emission of sPF, TPA50-sPF and Cz50-sPF

	(ps)	R^2
sPF	374	1.934
TPA50-sPF	132; 928; 4889	1.386
Cz50-sPF	245	1.109

F. Evaluating the stabilities of emission spectra in poly-spiros

Here we examine the color stability of Cz-TPA-sPF at various current density (from 0.2 mA/cm^2 to over 1000 mA/cm^2), the results are depicted in Fig.S6. As we can see, the emission color of Cz-TPA-sPF is quite stable during device operation, the EL spectrum remains blue emission even under the high current density, 1330 mA/cm^2. The above experimental results demonstrate that Cz-TPA-sPF is a stable blue emitting material.

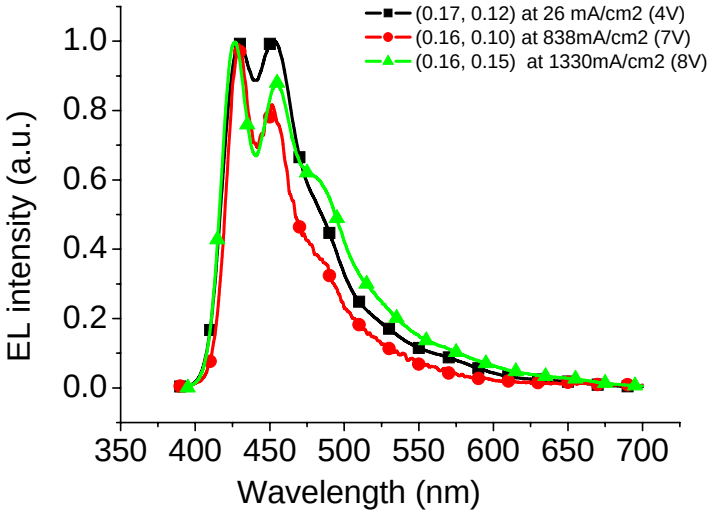

FIGURE S6 Electroluminescence spectra of Cz-TPA-sPF at various current densities.

We also evaluate the thermal stabilities of poly-spiros by recording the PL spectra after annealing the polymer film in air (180 °C for 2h). As shown in Fig.S7, the thermal treatment did not affect the PL spectra of poly-spiros. That is, no green-blue band emission was observed after the film was annealed at 180 °C for 2 h in air.

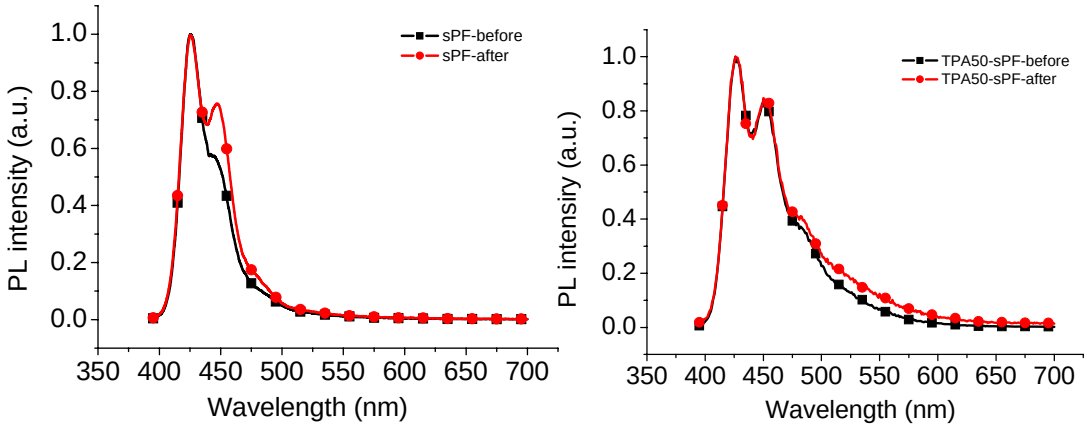

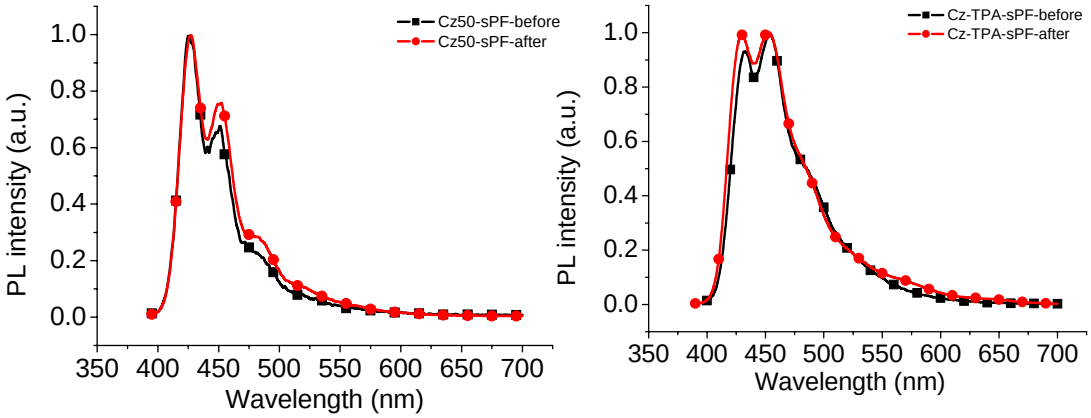

FIGURE S7 Thermal stabilities of poly-spiros after annealing at 180°C in air for 2 h.

G. Green Electroluminance from the Device with TPA-Cz-sPF :

FTIR measurement was performed on pristine TPA-Cz-sPF film and its spectrum is shown in Fig. S7(a). The Keto defect is not found in the pristine state (i.e. no Keto characteristic peak at 1725 cm^{-1} is found). However, additional green emission in PL spectrum appears as a shoulder (in range of 470-600 nm) as compared to the sPF (Fig. S8(b)), indicating that the green emission is not contributed from the chemical defect.

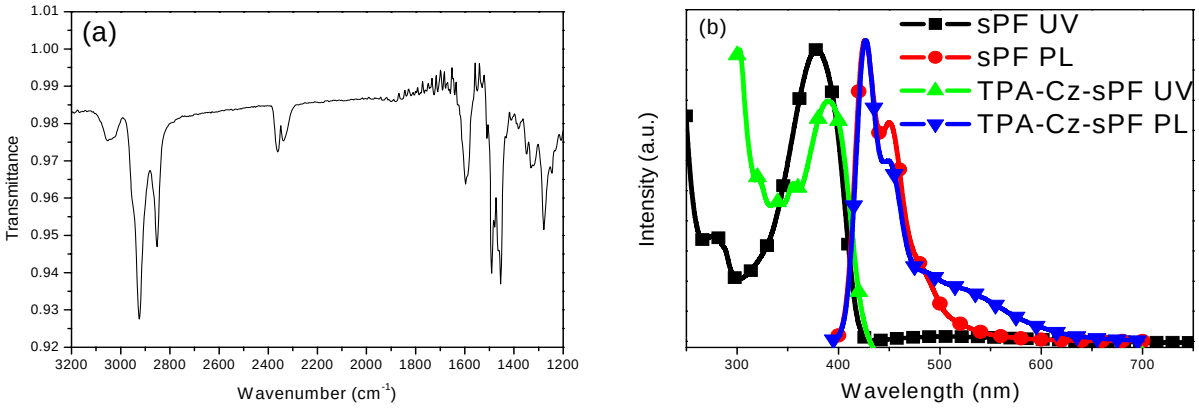

FIGURE S8 (a) FTIR measurement of TPA-Cz-sPF in its pristine film. (b) UV and PL of TPA-Cz-sPF and sPF in solid film state.

We further compare the PL and PLE spectra of TPA-Cz-sPF films from the devices before and after operation (i.e., after operation at 4V and 7V) to identify the origin of the green emission (by irradiating excitation light from the ITO side). For the used device, the emission intensity of the long-wavelength region (470-536 nm) is larger than that of the device before operation (Figure S9). The above result means that either exciplex (excimer) or aggregate might form after the device operation. However, in the PLE spectra, the long-wavelength tail (430-470 nm) remains unchanged before and after the operation, indicating that no aggregates are formed due to the absence of ground state interaction. Green component may be contributed by a formation of exciplex (or excimer) that can be further promoted by the electric field. [S7]

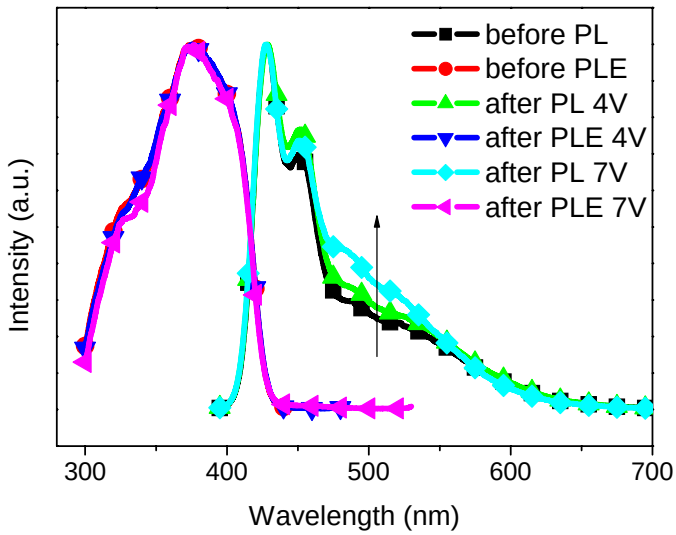

FIGURE S9 PLE (monitored at 480 nm and normalized at 388 nm) and PL (excited at 388 nm and normalized at 423 nm) spectra measurement from TPA-Cz-sPF based devices before and after operation. All spectra were measured by irradiating excitation light from the ITO side.

From the above experimental results, the green component in TPA-Cz-sPF can be observed in PL and can be further promoted under the electric field treatments; the green component is not from the chemical defect due to the absence of Keto characteristic peak at 1725 cm^{-1}. We can conclude that such green emission is not from aggregates (contributed from ground state interaction between these moieties) but from excimer or exciplex. Detailed investigation on the origin of this green component is in progress.

H. Detailed Characteristics of the Devices in Luminance and Current Density Versus Applied Voltage:

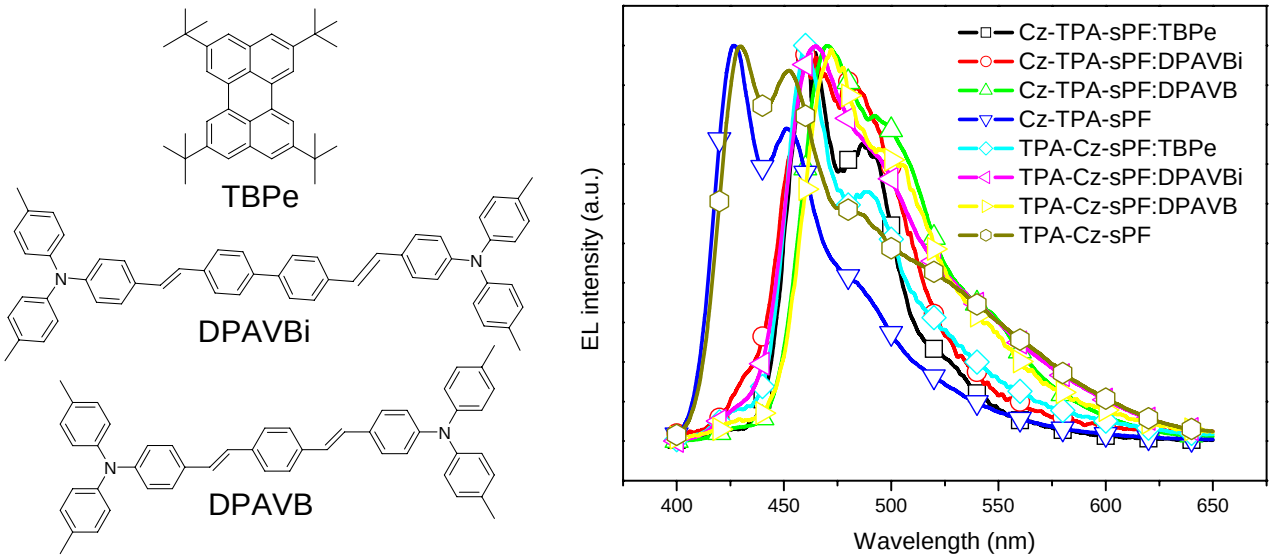

Figure S10 The chemical structures of dopants used in this study and their corresponding electroluminance spectra while doped into poly-spiro hosts.

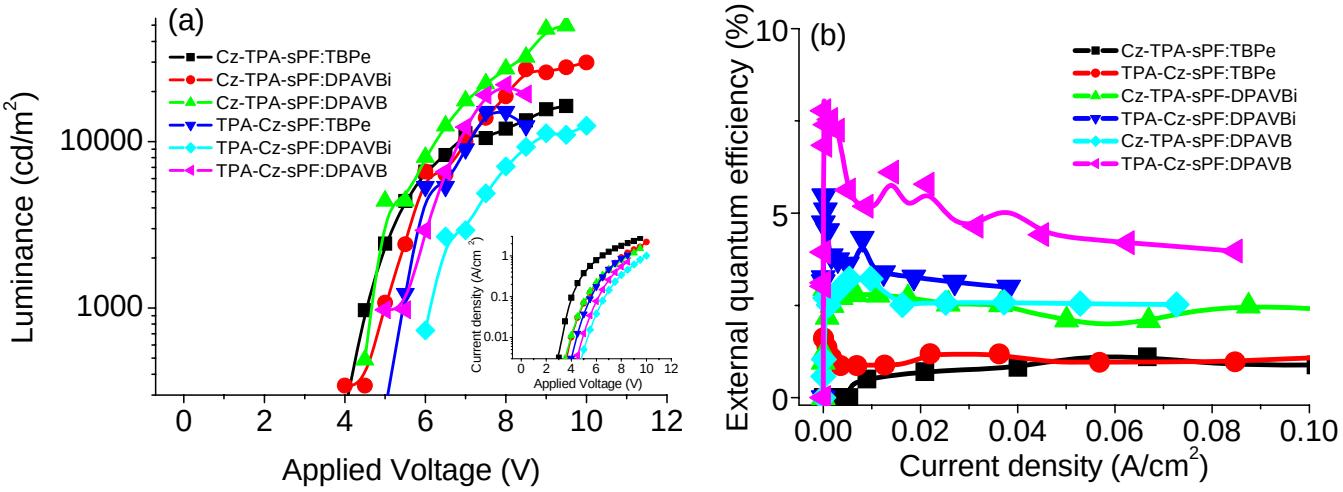

FIGURE S11 (a) characteristics of the PLEDs, ITO/PEDOT/poly-spiro with 2wt% dopant/CsF/Ca/Al, in luminance and current density versus applied voltage, (b) characteristics of the PLEDs, ITO/PEDOT/ poly-spiro with 2wt% dopant/CsF/Ca/Al, in external quantum efficiency versus current density.

I. A Comparison of our EL Devices with the Existing Blue PLEDs Based on Conjugated Polymers

Table S6. Comparison of our pure blue [a] device performance with others in the literature

Color	cd/m2	cd/A;%; lm/W	CIE	No. of layer	Data from
Pure BLUE	22,000	4.57; 4.54; 3.77	(0.16, 0.10)	1	This work
Pure BLUE	1700	2.5; 2; 1.57	(0.15, 0.14)	2	Ref. S8a
Pure BLUE	5000	2.02; 3.04; 0.94	(0.16, 0.07)	2	Ref. S8b
Pure BLUE	2870	1.5; 1.5; N.A.	(0.18, 0.11)	1	Ref. S8c
Pure BLUE	3137	1.42;1.06;N.A.	(0.15,0.15)	2	Ref. S8d
Pure BLUE	1000	0.82;1.74;N.A.	(0.15, 0.07)	2	Ref. S8e
Pure BLUE	5500	0.56;N.A.;N.A.	(0.15,0.05)	1	Ref. S8f

[a] CIE coordinate $x+y<0.3$; N.A. refers not available

Table S7. Comparison of our sky blue [a] device performance with others in the literature

Color	cd/m2	cd/A;%; lm/W	CIE	No. of layer	Data from
SKY BLUE	14,000	13.1; 7.53; 10	(0.19, 0.20)	1	This work
SKY BLUE	22,000	17.9; 8.32; 15.1	(0.18, 0.32)	1	This work (doped device)
SKY BLUE	N.A	11.5; N.A.; 5.5	(0.15, 0.30)	2	Ref. S9a
SKY BLUE	10,000	3.0;N.A; N.A	(0.16, 0.19)	1	Ref. S9b
SKY BLUE	9585	3.87; 2.07; 1.73	(0.15, 0.27)	2	Ref. S9c
SKY BLUE	1100	2.69; 1.62; 1.25	(0.15, 0.17)	2	Ref. S9d
SKY BLUE	2770	0.25; 0.52;N.A.	N.A.	1	Ref. S9e
SKY BLUE	250	0.5;N.A.;N.A.	(0.18,0.17)	1	Ref. S9f
SKY BLUE	2630	0.83;0.54;N.A.	(0.17,0.14)	1	Ref. S9g
SKY BLUE	4000	2.82;N.A.;1.31	(0.16,0.19)	N.A.	Ref. S9h
SKY BLUE	5500	2.33; 2.95;N.A.	(0.18, 0.14)	2	Ref. S9i
SKY BLUE	4080	N.A.;1.21;N.A.	(0.19,0.14)	1	Ref. S9j

[a] CIE coordinate x+y > 0.3, which appears as sky blue or greenish blue; N.A. refers not available

References

[S1]. C. F. Shu, R. Dodda, F. I. Wu, M. S. Liu, Jen. K.-Y. Alex, *Macromolecules* **2005,** *36,* 6698.

[S2]. Y. Wu, J. Li, Y. Fu, Z. Bo, *Org. Lett.* **2004,** *6,* 3485.

[S3]. X. Chen, J. L. Liao, Y. M. Liang, M. O. Ahmed, H. E. Tseng, S. A.Chen, *J. Am. Chem. Soc.* **2003,** *125,* 636.

[S4]. O. Kwon, S. Kwon, M. Jazbinsek, S. Lee, P. Guenter. *Polymer* **2005,** *46,* 10301.

[S5]. S.P. Huang, J. L. Liao, H. E. Tseng, T. H. Jen, J. Y. Liao, S. A. Chen, *Synth. Met.* **2006**, *156*, 949.

[S6]. T. Sumiyoshi, *Chem. Lett.* **1995,** *24,* 645.

[S7]. H. H. Lu, C. Y. Liu, T. H. Jen, J. L. Liao, H. E. Tesng, C. W. Huang, M. C. Hung, S. A. Chen, *Macromolecules* **2005,** *38,* 10829.

[S8]. (a) S. R. Tseng, S. Y. Li, H. F. Meng, Y. H. Yu, C. M.Yang, H. H. Liao, S. F. Horng, C. S Hsu,. *J. Appl. Phys.* **2007,** *101,* 084510. (b) F. I. Wu, P. I. Shih, C. F. Shu, Y. L. Tung, Y. Chi, *Macromolecules* **2005,** *38,* 9028. (c) E. Wang, C. I. Li, Y. Mo, Y. Zhang, G. Ma, W. Shi, J. Peng, W. Yang, Y. Cao, *J. Mater. Chem.* **2006,** 16, 4133. (c) Y. H. Niu, B. Chen, T. D. Kim, M. S. Liu, A. K. Y. Jen, *Appl. Phys. Lett.* **2004,** *85,* 5433. (d) H. J. Su, F. I. Wu, C. F.Shu, *Macromolecules* **2004,** *37,* 7197. (e) Y. H. Tseng, P. I. Shih, C. H. Chien, A. K. Dixit, Y. H. Liu, G. H. Lee, *Macromolecules* **2005,** *38,* 10055. (f) S. Qiu, L. Liu, B. Wang, F. Shen, W. Zhang, M. Li, Y. Ma, *Macromolecules* **2005,** *38,* 6782.

[S9]. (a) T. W. Lee, M. G. Kim, S. Y. Kim, S. H. Park, T. S. Oh, *Appl. Phys. Lett.* **2006,** *89,* 123505. (b) C. D. Muller, A. Falco, N. Reckefuss, M. Rojahn, V. Wiederhirn, P. Rudati, H. Frohne, O. Nuyen, H. Becker, K. Meerholz, *Nature* **2003,** *421,* 829. (c) H. J. Su, F. I.Wu, Y. H. Tseng, C. F. Shu, *Adv. Fun. Mater.* **2005,** 15, 1209. (d) M. Sun, Q. Niu, R.Yang, B. Du, R. Liu, W. Yang, J. Peng, Y. Cao, *European. Polym. J.*. **2007,** *43,* 1916. (d) F. Wu, S. Reddy, C. F. Shu, *Chem. Mater.* **2003,** *15,* 269. (e) J. Jacob, S. Sax, T. Riok, E. J. W. List, A. C. Grimsdale, K. Mullen, *J. Am. Chem. Soc.* **2005,** 126, 6987. (f) R. Liu, Y. Xiong, W. Zeng,; Z. Wu, B. Du, W. Yang, M. L. Sun, Y. Cao, *Macromol. Chem. Phys.* **2007,** *208,* 1503. (g) W. Wu, M. Inbasekarab, M. Hudack, D. Welsh, W. Yu, Y. Cheng, C. Wang, S. Kram, M. Tacey, M. Bernius, R. Fletcher, K. Kiszka, S. Munger, J. O'Brien, *Microelectonics. J.* **2004,** 35, 343. (h) R. Zhu, W. Y. Lai, H. Y. Wang, N. Yu, W. Wei, B. Peng, W. Huang, *Appl. Phys. Lett.* **2007,** *90,* 141909. (j) C. F. Shu, R. Dodda, F. I. Wu, M. S. Liu, A. K. Y. Jen, *Macromolecules* **2003,** 3*6,* 6698.